Tuning the pulse duration, spectral position and bandwidth of femtosecond pulses by the beam's penetration in an intracavity prism

N. Dimitrov, I. Stefanov, A. Dreischuh

Department of Quantum Electronics, Faculty of Physics, Sofia University, Sofia, Bulgaria

ABSTRACT

In this work we study the influence of the additional second- and third-order dispersion introduced in a femtosecond laser cavity by varying the beam's penetration into a prism of the double-pass intracavity prism compressor on the output pulse duration, as well as on the emission spectral bandwidth and its central wavelength. The theoretically calculated pulse durations are found to be in a good agreement with the respective experimental data from frequency-resolved optical gating and interferometric autocorrelation measurements.

Keyword list: femtosecond pulses, intracavity dispersion management, second-order dispersion, third-order dispersion, prism compressor, pulse compression, frequency-resolved optical gating, interferometric autocorrelation.

1. INTRODUCTION

Progress in ultrafast optics relies extensively on the development of ways to characterize and manipulate dispersion[1,2]. Generally, the phase φ can be expanded in a Taylor series around the central frequency ω_0 of the generated spectrum,

$$\varphi(\omega) = \varphi(\omega_0) + \frac{d\varphi}{d\omega}(\omega-\omega_0) + \frac{1}{2}\frac{d^2\varphi}{d\omega^2}(\omega-\omega_0)^2 + \frac{1}{6}\frac{d^3\varphi}{d\omega^3}(\omega-\omega_0)^3 + \dots , \quad (1)$$

where (left to right) the terms describe the phase at the carrier frequency ω_0, the group delay, the group-delay dispersion (GDD), the third-order dispersion (TOD) etc., respectively. It is worth mentioning that the group-velocity dispersion (GVD) is related to the second derivative of refractive index with respect to wavelength by

$$GVD = \frac{\lambda^3}{2\pi c^2}\left(\frac{d^2 n}{d\lambda^2}\right) \quad (2)$$

and, hence, the GDD is simply a product of the GVD with the length of the dispersive material. The *n*-th derivative of the phase function with respect to frequency $(d^n\varphi/d\omega^n)$ evaluated at a the central angular frequency of the spectrum ω_0 is measured in units of [rad^{1-n} fs^n], usually simplified to [fs^n], whereas the GVD is measured in [fs^2/cm]. In order to make effective use of already generated short optical pulses it is necessary to be able to deliver them undistorted to the experiment. The transition of a transform-limited ultrashort pulse emitted from a femtosecond laser through transparent optical media inevitably leads to temporal shift between the different spectral components due to the dispersion and, hence, to an undesired pulse broadening. For example, in the simplest case of an incoming Gaussian pulse of duration Δt the output pulse is broadened due to the GDD to

$$\Delta t_{out} = \sqrt{\Delta t^4 + 16\ln^2(2) GDD^2}\,/\,\Delta t \quad . \quad (3)$$

Inside a laser cavity each term (and derivative) in Eq. 1 is a sum of the terms introduced by the individual components. A reasonable rule of thumb is that the closer to the zero the second-order dispersion of the cavity (GDD, GVD), the shorter the generated pulse[3]. This rule breaks down as soon as very low dispersion regime is reached, since the third order dispersion (TOD) can no longer be neglected[4]. Instead of a prism sequences[5-11] specially designed chirped dielectric mirrors for high-accuracy compensation of the positive GDD are frequently used[12-16]. Prism pair in combination with double-chirped mirrors may balances the higher-order dispersion of the prism pair and, therefore, may flatten the average total group-delay dispersion in the laser cavity[17]. Precise dispersion management allows to reach the sub-two cycle regime[18-20].

It should be mentioned that pulse widening is important before amplifying short pulses in solid-state laser media[21] in order to avoid catastrophic damage of the components. In the chirped-pulse amplification approach[22,23] a short input pulse is temporally stretched before amplification and, after amplification, is recompressed to its Fourier-transform limit. The use of a stretcher can be avoided[24] if sufficiently large amount of dispersion is accumulated during the amplification process to prevent self-focusing but still compensation in SOD and TOD is needed in order to shorten the amplified pulses down to nearly the bandwidth limit.

Generally speaking[24], transparent optical materials have positive SOD and TOD, while double-pass prism compressors introduce negative SOD and TOD. The SOD of a grating compressor is negative, whereas its TOD is positive. Both types of compressors introduce negative fourth-order dispersion (FOD), but the FOD of an optical material can be either positive or negative. It is widely adopted[25] that only chirped mirrors allow for the compensation of a much more general spectral dependence of the dispersion unfortunately introducing it in discrete portions at each reflection.

2. DISPERSION BALANCE IN THE LASER OSCILLATOR

The optical scheme of the used femtosecond oscillator (*Ti:Light*, Quantronix) is shown in Fig. 1. The laser is pumped by the second-harmonic of a continuous-wave Nd:YVO_4 laser (λ_{pump} =532nm) and, for pump power of some 3W, delivers more than 200mW at 800 nm. Our aim is to study the possibility to tune the output pulse duration, the central wavelength of the spectrum and the bandwidth of the femtosecond pulses by changing the beam's penetration into the intracavity prism P2 without interrupting the mode locking.

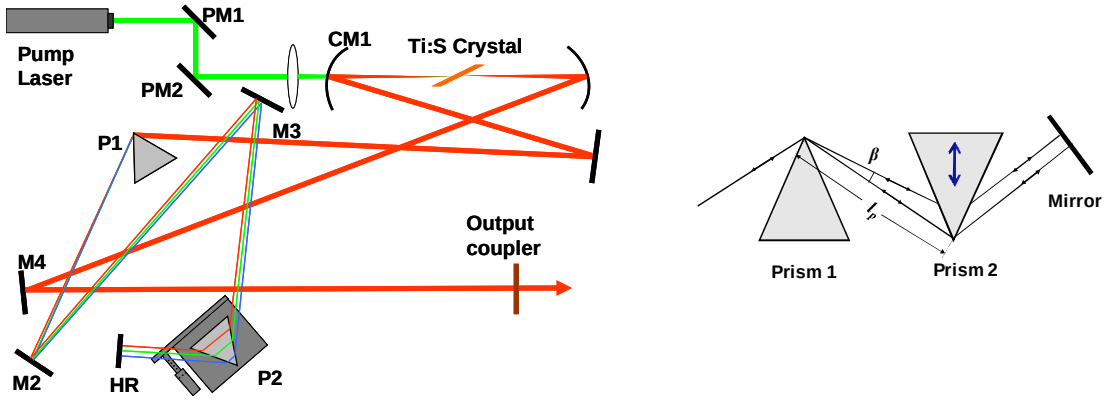

Fig. 1. (Left) Scheme of the laser oscillator. PM1, PM2 – pump mirrors; CM1, CM2-curved mirrors; M1…M3 – flat mirrors, P1, P2 – Brewster-cut quartz prisms of the double-pass intracavity prism compressor; HR – back high-reflection mirror. (Right) Stationary and movable prisms of the prism compressor and notations relevant to Eqs. 6.

Important for estimating the dispersion inside the cavity is the calculation of the SOD and TOD introduced by the prism compressor when the laser beam prism is penetrating to a different depth in the prism P2. The classical analyses[26-28] assume that the beam is passing through the apex of this prism and the respective results for the second and third derivatives of phase with respect to frequency are

$$\frac{d^2\varphi}{d\omega^2} = \frac{\lambda^3}{2\pi c^2}\frac{d^2P}{d\lambda^2} \tag{4}$$

and

$$\frac{d^3\varphi}{d\omega^3} = \frac{-\lambda^4}{4\pi^2 c^3}\left(3\frac{d^2P}{d\lambda^2} + \lambda\frac{d^3P}{d\lambda^3}\right)\ldots, \tag{5}$$

where the derivatives of the path P in the prism sequence are

$$\frac{d^2P}{d\lambda^2} = 4\left[\frac{d^2n}{d\lambda^2} + \left(2n - \frac{1}{n^3}\right)\left(\frac{dn}{d\lambda}\right)^2\right] l_p \sin(\beta) \tag{6a}$$

and

$$\frac{d^3P}{d\lambda^3} = 4\frac{d^3n}{d\lambda^3} l_p \sin(\beta) - 24\frac{dn}{d\lambda}\frac{d^2n}{d\lambda^2} l_p \cos(\beta) \quad . \tag{6b}$$

Analytic expressions for the fourth- and the fifth-order dispersions of crossed prisms pairs, both at arbitrary and Brewster-angle incidences are also known in the literature[29]. In Eqs. 6 l_p is the extreme (reference) ray that passes from apex to apex between the prisms and β is the angle of a particular ray with respect to the reference one.

In our experiments, however, we vary the penetration depth of the prism P2 (see Fig. 1) and deeper penetration means positive material dispersion for pulses propagating through this prism, which has to be correctly accounted for. We do this by using the more elaborate results of Zhang and co-authors[30-31] for the SOD and TOD

$$D2 = \frac{\lambda^3}{2\pi c^2} Q_2 \quad , \tag{7}$$

$$D3 = \frac{-\lambda^4}{2\pi^2 c^3}\left(3Q_2 + \lambda Q_3\right) \quad , \tag{8}$$

where

$$Q_2 = 4\left[\frac{d^2n}{d\lambda^2} + \left(2n - \frac{1}{n^3}\right)\left(\frac{dn}{d\lambda}\right)^2\right] d\tan\left(\frac{\alpha}{2}\right) - 8\left(\frac{dn}{d\lambda}\right)^2\left[l + d\tan\left(\frac{\alpha}{2}\right)\tan\left(\frac{\varepsilon}{2}\right)\right] \quad , \tag{9a}$$

$$Q_3 = 4\frac{d^3n}{d\lambda^3} d\tan\left(\frac{\alpha}{2}\right) - 24\frac{dn}{d\lambda}\frac{d^2n}{d\lambda^2}\left[l + d\tan\left(\frac{\alpha}{2}\right)\tan\left(\frac{\varepsilon}{2}\right)\right] \quad . \tag{9b}$$

In Eqs. 9 l and d are the distance between the prisms and the depth of penetration in the prism (P2, see Fig. 1), α is the prism apex angle, and ε is the beam deviation angle. As suggested[30-31], one can use the more convenient representation of the above results into separation-dependent term (proportional to l) and penetration-dependent term (proportional to d)

$$D_{2P} = D_{2l} l + D_{2d} d \quad , \tag{10a}$$

$$D_{3P} = D_{3l} l + D_{3d} d \quad , \tag{10b}$$

but in the rest of this paper we use the complete results given in Eqs.7-9.

At a central wavelength of 800 nm the 4 mm long Ti:Sapphire crystal introduces GVD of +56.6 fs^2/mm which, for one cavity roundtrip, means GDD=+452.8 fs^2. The respective value for the TOD for a double pass through the crystal is TOD=+331.2 fs^3. The prisms in our oscillator are made of fused silica, for which, at 800 nm, the refractive index is n=1.45332, GVD =+36.1 fs^2/mm, and TOD=+27.4 fs^3/mm. Due to the finite beam size the beam passes some 3.8 mm through the first prism P1 (see Fig. 1) which adds +274.4 fs^2 SOD and +208.2 fs^3 TOD. The prism separation l we kept unchanged during our measurements (l=52.8 cm). Depending on the penetration depth d of the beam into the material of prism P2, the dispersion of the prism compressor (the dispersion of the first prism excluded) varies from (GDD= - 857 fs^2, TOD= - 1025 fs^3) for the most shallow penetration $d=d_{\min}$=3 mm to (GDD= - 552 fs^2, TOD= - 806 fs^3) for the most deep penetration $d=d_{\max}$=6.2 mm. Quartz beamsplitter placed outside the cavity just behind the output mirror (not shown in Fig. 1) introduces additionally +180.5 fs^2 GDD and +137 fs^3 TOD. The overall *constant* dispersion accumulated in the active medium, the first prism P1 and in the beamsplitter is GDD = 907.7 fs^2 and TOD = 676.4 fs^3. In order to get the total dispersion, one should add the *variable* dispersion, introduced by the prism compressor (first prism P1 excluded). As already underlined, the total dispersion will depend on the penetration d of the beam into the material of the second prism P2.

We present the dispersion data using the so-called D2-D3 map[32,33], in which the SOD D2 is drawn as a horizontal coordinate, the TOD D3 - as a vertical, and all sources of cavity dispersion are plotted as vectors.

3. EXPERIMENTAL DATA AND ANALYSIS OF THE RESULTS

The translation stage on which the prism P2 is mounted provides the opportunity to control the beam's penetration depth into the prism material. At each position, without any interruption in the mode locking, we characterized the output pulses by a frequency-resolved optical gating device (*GRENOUILLE*, Swamp Optics), by a home-build interferometric autocorrelator, and by a fiber-coupled spectrometer (Ocean Optics). The stability of the mode-locked pulse train was continuously monitored by an oscilloscope.

For each particular value of the prism penetration depth the estimated values of the GDD and TOD we used to numerically calculate the pulse shape and its width. These results we then compared with these from the

measurements as shown in Fig. 3. As seen, the less the prism penetration in the laser beam, the less the duration of the emitted pulse, which is due to the increased (as an absolute value) negative SOD and TOD of the prism compressor (see the arrows in the third quadrant on Fig. 2). Both experimental and theoretical curves show qualitatively similar nonlinear behavior vs. prism penetration depth. The three frames to the right of Fig. 3 are FROG traces at three different positions indicated also on the graph. Qualitatively, the pulses shown in frames A and B are approximately equal in time width, but frame C is gradually broader, actually corresponding to the longest pulse we could generate in this way. In Fig. 4 we show two examples of autocorrelation curves recorded with standard second-harmonic (SH) interferometric autocorrelator in the case of strongly (left; SOD= +264 fs^2; TOD= -196 fs^3) and moderately chirped (right; SOD= + 142 fs^2; TOD= - 284 fs^3) femtosecond pulses. The smooth solid curves show the envelopes of the calculated autocorrelation traces adjusted to the experimental ones in a way to smoothly fit to the background SH autocorrelation signal. In this way we deduce pulse durations of 88 fs and 57 fs, respectively, for both cases (see Fig. 4). These results are in a qualitative agreement with the values measured by the FROG device (40 fs and 36 fs, respectively; calculated values – 44.3 fs and 30 fs, respectively).

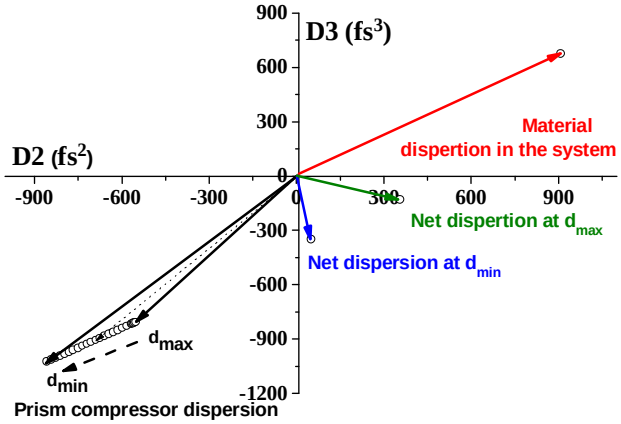

Fig. 2. (Color online) Vector diagram representing the portion of the dispersion introduced in the cavity by the prism compressor, when varying the position ***d*** of the prism P2- black arrows. GDD and TOD from all other cavity elements remain unchanged. Blue and green lines - net values of the overall cavity dispersion for the two limiting positions ***d*** of the moving prism.

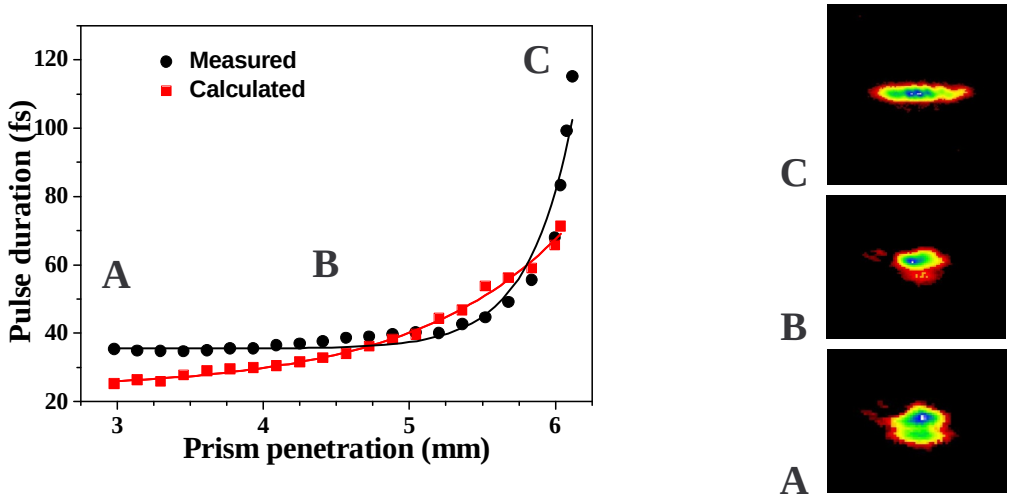

Fig. 3. Dependence of the output pulse duration on the prism penetration due to the changed net intracavity dispersion. Black curve (circles) - experimental results; red curve (squares) – numerical data. Insets - measured FROG traces at specific positions.

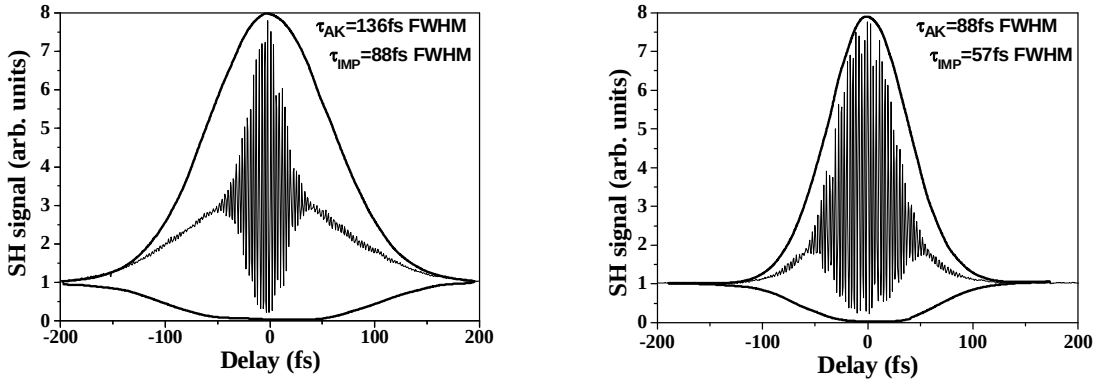

Fig. 4. Interferometric second-harmonic autocorrelation curves demonstrating strongly (left; SOD= +264 fs^2; TOD= -196 fs^3) and moderately chirped (right; SOD= + 142 fs^2; TOD= - 284 fs^3) femtosecond pulses with durations of 88 fs and 57 fs, respectively. Smooth solid curves – calculated envelopes of the autocorrelation traces.

As mentioned, at large penetrations of the prism in the beam we estimated large positive SOD and relatively small negative TOD (see arrow net dispersion at d_{max} in Fig. 2). In this case we measured one of the longest pulses in this experiment (~120 fs) with spectra spanning over some 88 nm. It is clearly seen that these pulses are by far not transform-limited but have potential for compression outside the cavity. The spectral width of the shortest pulses of 35.4 fs duration (full width at half maximum) we measured to be 30.3 nm, which corresponds to a time-bandwidth product, which is 1.4 times larger that the transform-limit.

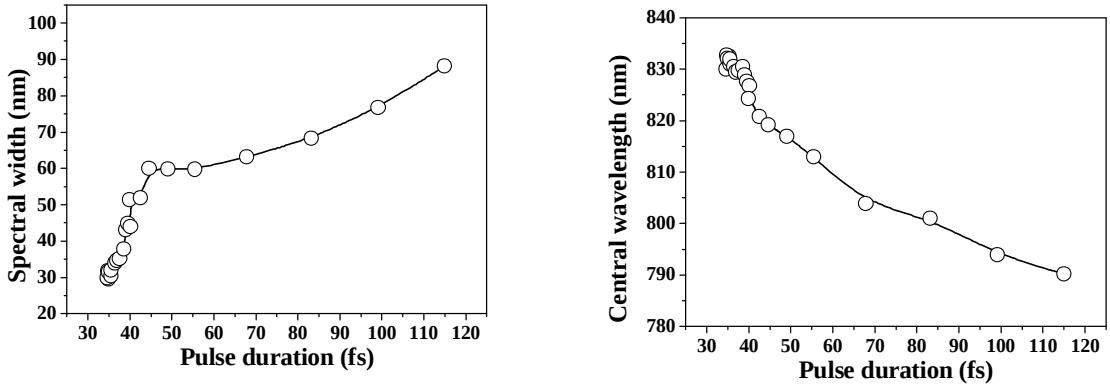

Fig. 5. Spectral width (left) and emission central wavelength (right) for the respective pulse durations measured with the frequency-resolved optical gating equipment.

We did not change intentionally the prism angular position but its penetration in the beam (and the respective SOD and TOD) only. The observed red shift of the central wavelength of the pulse spectrum when the prism is moved out of the beam (and the pulses get shorter) is, however, clearly seen in the right graph in Fig. 5. At this stage we refrain from speculating on the reasons for this but would like to direct the reader's attention to the experimental data shown in Fig. 6. The mean output power (and the energy of each individual pulse emitted) from the oscillator monotonically increases with decreasing the pulse duration, which can be attributed, qualitatively, to the changes in the strength of the Kerr lens in the active medium and to changes in the mode-matching of the pump and the generated beam inside the Ti:Sapphire crystal. It is possible that this causes a slight change in the beam's angular position on the prisms and slightly changes also the wavelength, at which the Brewster input condition is fulfilled and the reflection losses are at minimum. Moreover, in the presented analysis we accounted for the material dispersion of a laser crystal only, ignoring the angular dispersion arising from the different paths in the resonator

traversed by the different wavelength rays in the laser crystal when incidence is not normal to the surface[34]. This angular dispersion should be accounted for in the future analyses.

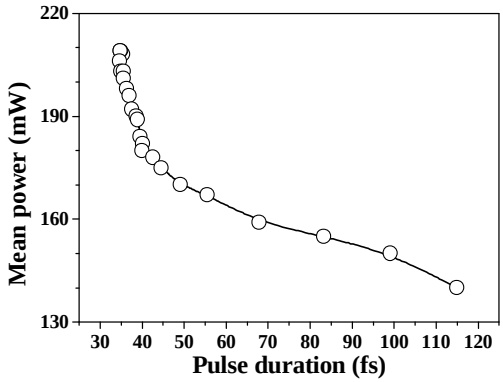

Fig. 6. Variation of the mean output power with the pulse duration when the prism penetration is changed.

5. CONCLUSION

In view of the above we can state that the controllable change of the penetration of one of the prisms constituting the inracavity prism compressor into the laser beam is a simple way to change the dispersion inside the cavity thus changing the duration of the emitted pulses. Shorter pulses are found to have larger pulse energies. This tuning approach allows also to easily tune the central wavelength and the bandwidth of the emitted pulses if needed. Further theoretical work is under way to better quantitatively describe the observed tendencies.

6. ACKNOWLEDGMENTS

This work was supported by the Science Fund of the Sofia University (grant 080/2010) and by the NSF-Bulgaria (grants DO-02-0114/2008 and DRNF-02-8/2009).

7. REFERENCES

[1] Walmsley, I., Waxer, L., and Dorrer, C., "The role of dispersion in ultrafast optics," Rev. Sci. Instrum. **72**, 1-29 (2001).

[2] Backus, S., Durfee III, C. G., Murnane, M. M., and Kapteyn, H. C., "High power ultrafast lasers," Rev. Sci. Instrum. **69**, 1207-1223 (1998).

[3] Haus, H. A., Fujimoto, J. G., and Ippen, E. P., "Structures for additive pulse mode locking," J. Opt. Soc. Am. B **8**, 2068–2076 (1991).

[4] Santagiustina, M., "Third-order dispersion radiation in solid-state solitary lasers," J. Opt. Soc. Am. B **14**, 1484-1495 (1997).

[5] Spence, D. E., Kean, P. N., and Sibbett, W., "60-fsec pulse generation from a self-mode locked Ti:sapphire laser," Opt. Lett. **16**, 42–44 (1991).

[6] Sarukura, N., Ishida, Y., and Nakano, N., "Generation of 50-fsec pulses from a pulse-compressed, cw, passively modelocked Ti:sapphire laser," Opt. Lett. **16**, 153–155 (1991).

[7] Keller, U., tHooft, G. W., Knox, W. H., and Cunningham, J. E., "Femtosecond pulses from a continuously self-starting passively mode-locked Ti:sapphire laser," Opt. Lett. **16**, 1022–1024 (1991).

[8] Spielmann, Ch., Curley, P. F., Brabec, T., Wintner, E., and Krausz, F., "Generation of sub-20 fs mode locked pulses from a Ti:sapphire laser," Electron. Lett. **28**, 1532–1533 (1992).

[9] Asaki, M. T., Huang, C. P., Harvey, D., Zhou, J., Nathel, H., Kapteyn, H. C., and Murnane, M. M., "11 femtosecond pulses from a modelocked Ti:sapphire laser," Opt. Photonics News **5**, 12 (1992).

[10] Zhou, J., Taft, G., Huang, C. P., Murnane, M. M., Kapteyn, H. C., and Christov, I. P., "Pulse evolution in a broadbandwidth Ti:sapphire laser," Opt. Lett. **19**, 1149–1151 (1994).

[11] Spielmann, Ch., Curley, P. F., Brabec, T., and Krausz, F., "Ultrabroad-band femtosecond lasers," IEEE J. Quant. Electron. **30**, 1100–1114 (1994).
[12] Stingl, A., Spielmann, Ch., Krausz, F., and Szipocs, R., "Generation of 11-fs pulses from a Ti:sapphire laser without the use of prisms," Opt. Lett. **19**, 204–206 (1994).
[13] Stingl, A., Lenzner, M., Spielmann, Ch., Krausz, F., and Szipocs, R., "Sub-10-fs mirror-dispersion-controlled Ti:sapphire laser," Opt. Lett. **20**, 602–604 (1995).
[14] Kasper A. and Witte, K. J., "10-fs pulse generation from a unidirectional Kerr-lens mode locked Ti:sapphire laser,"Opt. Lett. **21**, 360–362 (1996).
[15] Xu, L., Spielmann, Ch., and Krausz, F., "Ultrabroadband ring oscillator for sub-10-fs pulse generation," Opt. Lett. **21**, 1250–1252 (1996).
[16] Mayer, E. J., Möbius, J., Euteneuer, A., and Rühle, W. W., Szipocs, R., "Ultrabroadband chirped mirrors for femtosecond lasers," Opt. Lett. **22**, pp. 528-530 (1997).
[17] Jung, I. D., Kärtner, F. X., Matuschek, N., Sutter, D. H., Morier-Genoud, F., Zhang, G., Keller, U., Scheuer, V., Tilsch, M., and Tschudi, T., "Self-starting 6.5-fs pulses from a Ti:sapphire laser," Opt. Lett. **22**, 1009-1011 (1997)).
[18] Morgner, U., Kärtner, F. X., Cho, S. H., Chen, Y., Haus, H. A., Fujimoto, J. G., and Ippen, E. P., "Sub-two cycle pulses from a Kerr-lens mode-locked Ti:sapphire laser," Opt. Lett. **24**, 411–413 (1999).
[19] Chen, Y., Kärtner, F. X., Morgner, U., Cho, S. H., Haus, H. A., Ippen, E. P., and Fujimoto, J. G., " Dispersion-managed mode locking," J. Opt. Soc. Am. B **16**, 1999-2004 (1999).
[20] Sander, M. Y., Birge, J., Benedick, A., Crespo, H. M., and Kärtner, F. X., "Dynamics of dispersion managed octave-spanning titanium:sapphire lasers," J. Opt. Soc. Am. B **26**, 743-749 (2009).
[21] Salin, F., Squier, J., and Mourou, G., "Large temporal stretching of ultrashort pulses," Appl. Opt. **31**, 1225-1228 (1992).
[22] Strickland D. and Mourou, G., "Compression of amplified chirped optical pulses," Opt. Commun. **56**, 219-221 (1985).
[23] Maine, P., Strickland, D., Bado, P., Pessot, M., and Mourou, G., "Generation of ultrahigh peak power pulses by chirped pulse amplification," IEEE J. Quantum Electron. **24**, 398-403 (1988).
[24] Lindner, F., Paulus, G. G., Grasbon, F., Dreischuh, A., and Walther, H., "Dispersion control in a 100-kHz-repetition-rate 35-fs Ti:sapphire regenerative amplifier system," IEEE J. Quant. Electron. **QE-38**, 1465-1470 (2002).
[25] Steinmeyer, G., "Femtosecond dispersion compensation with multilayer coatings: toward the optical octave," Appl. Opt. **45**, 1484-1490 (2006).
[26] Fork, R. L., Martinez, O. E., and Gordon, J. P., "Negative dispersion using pairs of prisms," Opt. Lett. **9**, 150-152 (1984).
[27] Fork, R. L., Brito Cruz, C. H., Becker, P. C., and Shank, C. V., "Compression of optical pulses to six femtoseconds by using cubic phase compensation," Opt. Lett. **12**, 483-485 (1987).
[28] Kostenbauder, A. G., "Ray-pulse matrices: **A** rational treatment for dispersive optical systems," IEEE J. Quant. Electron. **QE-26**, 1148-1157 (1990).
[29] Cojocaru, E., "Analytic Expressions for the Fourth- and the Fifth-Order Dispersions of Crossed Prisms Pairs," Appl. Opt. **42**, 6910-6914 (2003).
[30] Zhang, Z. and Yagi, T., "Observation of group delay dispersion as a function of the pulse width in a mode locked Ti:sapphire laser," Appl. Phys. Lett. **63**, 2993-2995 (1993).
[31] Zhang, Z., Toizuka, K., Itatani, T., Kobayashi, K., Sugaya, T., Nakagawa, T., "Femtosecond Cr:Forsterite laser with mode locking initiated by a quantum-well saturable absorber," IEEE J. Quant. Electron. **QE-33**, 1975-1981 (1997).
[32] Naganuma, K. and Mogi, K., "50-fs pulse generation directly from a colliding-pulse mode-locked Ti:sapphire laser using an antiresonant ring mirror," Opt. Lett. **16**, 738–740 (1991).
[33] Yamashita, M., Kaga, S., and Torizuka, K., "Chirp-compensation cavity mirrors with minimal third-order dispersion for use in a femtosecond pulse laser," Opt. Commun. **76**, 363–368 (1990).
[34] Zhang, R., Ma, J., Pang, D., Sun, J., and Wang, Q., "Spatial chirp and angular dispersion of a laser crystal for a four-mirror cavity Kerr-lens mode-locked laser," Appl. Opt. **43**, 2184-2191 (2004).